Plant Physiol. (1990) 93, 915–923
0032-0889/90/93/0915/09/$01.00/0

Received for publication December 7, 1989
Accepted March 19, 1990

Abscisic (ABA)-Aldehyde Is a Precursor to, and 1′,4′-*trans*-ABA-Diol a Catabolite of, ABA in Apple[1]

Christopher D. Rock and Jan A. D. Zeevaart*

Michigan State University-Department of Energy Plant Research Laboratory, Michigan State University, East Lansing, Michigan 48824-1312

ABSTRACT

Previous ^{18}O labeling studies of abscisic acid (ABA) have shown that apple (*Malus domestica* Borkh. cv Granny Smith) fruits synthesize a majority of [^{18}O]ABA with the label incorporated in the 1′-hydroxyl position and unlabeled in the carboxyl group (JAD Zeevaart, TG Heath, DA Gage [1989] Plant Physiol 91: 1594–1601). It was proposed that exchange of ^{18}O in the side chain with the medium occurred at an aldehyde intermediate stage of ABA biosynthesis. We have isolated ABA-aldehyde and 1′-4′-*trans*-ABA-diol (ABA-*trans*-diol) from ^{18}O-labeled apple fruit tissue and measured the extent and position of ^{18}O incorporation by tandem mass spectrometry. ^{18}O-Labeling patterns of ABA-aldehyde, ABA-*trans*-diol, and ABA indicate that ABA-aldehyde is a precursor to, and ABA-*trans*-diol a catabolite of, ABA. Exchange of ^{18}O in the carbonyl of ABA-aldehyde can be the cause of loss of ^{18}O from the side chain of [^{18}O]ABA. Results of feeding experiments with deuterated substrates provide further support for the precursor-product relationship of ABA-aldehyde → ABA → ABA-*trans*-diol. The ABA-aldehyde and ABA-*trans*-diol contents of fruits and leaves were low, approximately 1 and 0.02 nanograms per gram fresh weight for ABA-aldehyde and ABA-*trans*-diol, respectively, while ABA levels in fruits ranged from 10 to 200 nanograms per gram fresh weight. ABA biosynthesis was about 10-fold lower in fruits than in leaves. In fruits, the majority of ABA was conjugated to β-D-glucopyranosyl abscisate, whereas in leaves ABA was mainly hydroxylated to phaseic acid. Parallel pathways for ABA and *trans*-ABA biosynthesis and conjugation in fruits and leaves are proposed.

Evidence now strongly favors the indirect pathway of ABA biosynthesis from carotenoids. First, carotenoid biosynthetic mutants of maize are ABA-deficient (18), and fluridone, a specific inhibitor of carotenoid biosynthesis, inhibits ABA biosynthesis (8, 13). Second, heavy oxygen is incorporated from $^{18}O_2$ into the side chain of ABA during stress-induced biosynthesis, suggesting oxidative cleavage of a large precursor pool that contains oxygen functions on the ring (6, 7). Third, Li and Walton (14) have provided evidence that 9-*cis*-violaxanthin and 9′-*cis*-neoxanthin are precursors to ABA in dark-grown bean leaves. They showed a reduction in the levels of these two xanthophylls during water stress, with a concomitant increase in ABA and its catabolites PA[2] and dihydrophaseic acid, on a mole:mole basis. In contrast to higher plants, fungi synthesize ABA through α- and γ-ionylidene intermediates (29).

Xanthoxin is an apocarotenoid and a probable intermediate in ABA biosynthesis (22, 24). ABA-aldehyde has been postulated as the immediate precursor of ABA because the ABA-deficient tomato mutants *flacca* and *sitiens* are unable to convert xanthoxin or ABA-aldehyde to ABA *in vivo* (21, 25) or *in vitro* (23). ABA-*trans*-diol is an endogenous compound of plants and has been proposed as both a precursor to (20, 21), and a catabolite of ABA (26).

Zeevaart *et al.* (30) reported that ripe avocado and apple fruits, in contrast to stressed leaves, incorporated ^{18}O predominantly into the 1′-hydroxyl position of ABA. The apparent conflict of these results with the indirect pathway was reconciled by hypothesizing an exchange of ^{18}O label in the side chain carbonyl with water at an aldehyde intermediate stage of ABA biosynthesis. The present work was undertaken to determine if ABA-aldehyde is an endogenous compound in apple and could be the cause of the unusual ABA ^{18}O-labeling patterns in fruits. We also investigated the role of ABA-*trans*-diol in ABA biosynthesis.

MATERIALS AND METHODS

Plant Material

Young, fully expanded apple (*Malus domestica* Borkh. cv Mutsu) leaves were frozen in liquid N_2, or allowed to lose 12% fresh weight and subsequently incubated in 20% $^{18}O_2$:80% N_2 (v/v) for 12 or 24 h as previously described (7). The cultivars Granny Smith and Mutsu were used in post-harvest apple fruit experiments. Immature apple fruits were approximately 110 d post-anthesis. Alternatively, Mutsu apple fruits stored approximately 150 d under hypobaric conditions (0.05 atm at 0 °C to prevent ripening) were used. Cortical tissue (skin and core excised) was frozen or sliced into wedges and incubated with $^{18}O_2$ or exposed to air for 48

[1] Supported by the U.S. Department of Energy under contract DE-AC02-76ERO-1338, by the National Institutes of Health grant DRR00480 to the MSU-NIH Mass Spectrometry Facility, by National Science Foundation grant DMB-8703847 to J. A. D. Z., and by a Monsanto Graduate Fellowship to C. D. R.

[2] Abbreviations: PA, phaseic acid; ABA-GE, β-D-glucopyranosyl abscisate; ABA-*trans*-diol, 1′-4′-*trans*-ABA-diol; ECD, electron capture detection; EI, electron impact; FID, flame ionization detection; fr, fresh; M^-, odd electron negative molecular ion; Me-, methyl ester; MS-MS, GLC-NCI-collisionally activated dissociation-tandem mass spectroscopy; NCI, negative chemical ionization; PCI, positive chemical ionization; SIM, selected ion monitoring; *t-*, *trans*.

h before freezing. O_2 consumption and ethylene evolution were measured as described elsewhere (6, 12).

For feeding experiments, a 10 μM solution of deuterated substrate (approximately 2 μg/g fresh weight) in 2% (w/v) KCl plus 0.05% (v/v) Tween 20 (1) was vacuum-infiltrated and incubated at room temperature in the dark for 24 or 48 h. Control tissue was autoclaved for 20 min before incubation with substrate for 48 h.

Extraction and Purification of Metabolites

Frozen tissue was extracted overnight at 4 °C in acetone plus 0.01% (w/v) 2,6-di-*tert*-butyl-4-methylphenol and 0.25% (v/v) glacial acetic acid. The extract was drawn off and the tissue homogenized in an additional volume of extraction solvent with a Polytron (Brinkmann Instruments). The homogenate was filtered and 30 mL 1.0 M phosphate buffer (pH 8.3) was added to the combined fractions. The acetone was evaporated using a rotary evaporator at 35 °C and the aqueous extract adjusted to pH 7.2 with 6 N KOH. The extracts were filtered through a cellulose membrane to remove precipitates. With leaf extracts, Chl and lipids were removed by partitioning one to three times with an equal volume of hexanes. Measurement of the partition coefficient of an ABA-aldehyde standard indicated less than 8% loss from the aqueous fraction by partitioning with one volume of hexanes, and greater than 90% extraction of ABA-aldehyde from the aqueous fraction with one volume of ethyl acetate or diethyl ether (data not shown). The aqueous extract was partitioned three times with an equal volume of ethyl acetate to give the neutral fraction containing ABA-aldehyde. The aqueous phase was adjusted to pH 3.0 with 6 N HCl and partitioned four times with one volume of ethyl acetate to give the acidic fraction containing ABA, ABA-*trans*-diol, PA, and a portion of the ABA-GE (4). The organic fractions were taken to dryness under vacuum or N_2, and were further purified by HPLC.

ABA, ABA-GE, and PA in the acidic fraction were separated by reverse phase HPLC as previously described (6, 30). ABA-*trans*-diol coeluted with ABA and *t*-ABA from 23.5 to 26.5 min. The ethanol from the eluates was evaporated and the remaining water was removed by lyophilization. ABA-aldehyde from leaf neutral fractions was also purified using the same reverse phase HPLC conditions as described above; it eluted from 21 to 25 min. The ethanol was evaporated and an equal volume of 1.0 M phosphate buffer (pH 8.3) was added; the ABA-aldehyde was then partitioned four times into equal volumes of diethyl ether and dried under N_2 for normal phase HPLC. Apple fruit extracts did not require reverse phase HPLC for ABA-aldehyde purification.

The ABA plus ABA-*trans*-diol fraction was methylated with ethereal diazomethane and purified by normal phase HPLC with a μPorasil 30 × 0.4 cm column (Waters Associates). Elution was with a gradient of ethyl acetate in hexanes from 10 to 50% in 20 min at 2.0 mL/min. UV absorbance was monitored at 270 nm. Me-ABA was collected from 14.9 to 17.6 min, and Me-ABA-*trans*-diol from 18.8 to 21 min.

The fraction containing ABA-GE and PA was hydrolyzed with 2 N NH_4OH for 2 h at 60 °C to yield free ABA. The samples were dried, methylated and purified by the same HPLC system as for Me-ABA and Me-ABA-*trans*-diol, except a gradient of 10 to 60% ethyl acetate in hexanes in 10 min was used. Me-ABA and Me-*t*-ABA were collected from 12 to 13.8 min, and Me-PA from 14.5 to 16.5 min. ABA-aldehyde was purified using the same conditions, except UV absorbance was monitored at 282 nm. ABA-aldehyde was collected from 14.5 to 16.5 min. ABA-alcohol fractions were also collected from 18.5 to 21 min.

Quantifications

ABA-aldehyde and ABA-*trans*-diol were quantified by the method of isotope dilution (17) using deuterium-labeled internal standards. [$^2H_6$]ABA-aldehyde was synthesized by exchange of the ring hydrogens of ABA-alcohol in 1 N NaOD for 2 d, followed by oxidation in chloroform with manganese oxide IV (10) to [$^2H_6$]ABA-aldehyde. [$^2H_7$]ABA-*trans*-diol was synthesized by reduction of [$^2H_6$]ABA with sodium borodeuteride (11) and purified by reverse phase semipreparative HPLC. Deuterated standards were quantified by GLC-FID and GLC-ECD for ABA-aldehyde and Me-ABA-*trans*-diol, respectively, using standard curves of the unlabeled compounds. Quantification of ABA-aldehyde and Me-ABA-*trans*-diol standards was confirmed by UV absorbance in ethanol at 285 and 262 nm, using a molar extinction coefficient of 25,000 and 20,000, respectively (11) (C.D. Rock, unpublished observations). As determined by GLC-NCI-MS, the [$^2H_6$]ABA-aldehyde internal standard contained trace amounts of unlabeled ABA-aldehyde and was 56% hexadeutero-labeled. The [$^2H_7$]ABA-*trans*-diol was 60% heptadeutero-labeled with a trace of unlabeled compound. A calibration curve was made using various amounts of unlabeled and [$^2H_6$]ABA-aldehyde. A linear NCI-SIM response for m/z = 248 and 254 was observed when molar ratios of unlabeled ABA-aldehyde to [$^2H_6$]ABA-aldehyde were greater than 0.2, indicating that reliable measurements could be made when deuterated standard was added to extracts within a factor of five of the endogenous concentration of compound.

ABA, ABA-GE, and PA were quantified by GLC-ECD and addition of ^3H-labeled standards to correct for losses during extraction and purification (5). Percent recoveries for ABA and PA averaged approximately 50%, and typically 15% for ABA-GE because only a small fraction partitioned into the organic phase (4). In experiments with apple leaves where the entire extract was lyophilized instead of partitioned, ABA-GE recoveries were typically 50%.

MS

GLC-NCI-MS and GLC-NCI-SIM were performed on a JEOL AX-505H double focusing mass spectrometer equipped with a Hewlett-Packard 5890 gas chromatograph and a direct source inlet. The column used was a DB-1 capillary (30 m × 0.25 mm, film thickness 1.0 μm; or 30 m × 0.326 mm, film thickness 0.25 μm; J&W Scientific, Inc., Rancho Cordova, CA) injected in splitless mode with He as the carrier gas (flow rate 2.5 mL/min). GLC conditions were: oven temperature programmed from 50 to 180 °C at 35 °C/min, followed immediately by a temperature gradient from 180 to 260 °C at

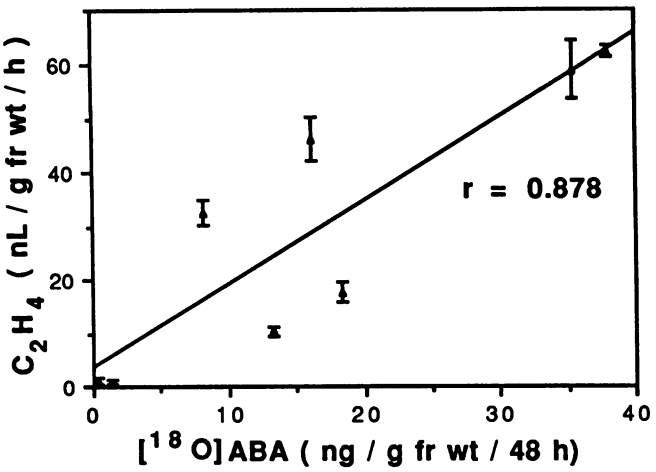

Figure 1. Relationship between the rate of ethylene evolution and ABA biosynthesis in Mutsu apple fruit. Cortical tissue from postharvest apples of varying degrees of ripeness was incubated 48 h under $^{18}O_2$. The content of [^{18}O]ABA was calculated from ABA levels measured by GLC-ECD multiplied by the percentage of [^{18}O]ABA enrichment in the same samples measured by GLC-NCI-SIM of M^-. Ethylene measurements ± SE.

10 °C/min. Methane was used as the reagent gas for NCI and PCI.

MS-MS was performed on a Finnegan TSQ 70 triple quadrupole mass spectrometer as described (30) with modifications. The collision energy in the second quadrupole was 9 eV for ABA-aldehyde, 2 eV for Me-ABA-*trans*-diol, and 3 eV for Me-ABA with an O_2 pressure of 0.19 Pa.

For analysis of mass spectral data, ion intensity values were normalized by subtracting the naturally abundant ^{13}C and ^{18}O isotope contributions. To express ^{18}O label incorporation into the side chain of ABA and metabolites as a percentage of total ^{18}O incorporation, the relative abundance of M^-, $(M + 2)^-$, $(M + 4)^-$, and $(M + 6)^-$ was measured by GLC-NCI-SIM and the percent of total [^{18}O]ABA for each M^- calculated. The percent ^{18}O enrichment of the side chain was measured by MS-MS. The product of these two measurements for each respective M^- yields the incorporation into the side chain as a percent of total ^{18}O incorporation.

The amount of ^2H-labeled product synthesized in feeding experiments was calculated from the ratio of deuterated to endogenous metabolite measured by GLC-SIM and multiplied by the amount of the endogenous compound measured by GLC-ECD of control tissue frozen at the beginning of the experiment. The extent of ^2H exchange by [^{2}H]ABA-GE during hydrolysis was small (data not shown), and resulted in a slight underestimation of [^{2}H]ABA-GE quantities in feeding experiments.

Chemicals

$^{18}O_2$ (97–98% enrichment) was purchased from Cambridge Isotopes Laboratories (Woburn, MA). Synthetic (±)-ABA-aldehyde and (±)-ABA-alcohol were gifts of Dr. M. Soukup, Hoffmann-LaRoche Inc., Basel, Switzerland.

RESULTS

ABA Biosynthesis in Fruits and Leaves

The relationship between ethylene evolution and ABA biosynthesis as measured by ^{18}O incorporation in postharvest Mutsu fruit tissue is shown in Figure 1. Although the data do not establish a causal relationship between ethylene production and ABA biosynthesis, the two biosynthetic processes are clearly linked. The postharvest increase in ABA biosynthesis was related to the ripening stage of the fruits. Each fruit began its climacteric at a different time, between 5 and 30 d after harvest, presumably due to the slightly different stage of ripening of each individual fruit. With apple fruits stored under hypobaric conditions, ethylene evolution began immediately after removal from storage and thus the fruits were synchronized with respect to ABA biosynthesis (data not shown). A correlation between the climacteric and ABA levels has been reported in avocado fruits (2).

Results on the biosynthesis and catabolism of ABA in fruits and water-stressed leaves are shown in Table I. Fruit tissue had a 10-fold lower rate of ABA biosynthesis than stressed leaves on a fresh weight basis. ABA levels averaged 200 ng/g fresh weight in these fruits and decreased about 70% during the labeling period with a concomitant increase in ABA-GE. In stressed leaves the ABA content was initially 360 ng/g fresh weight and increased approximately 50% during 24 h under $^{18}O_2$. No *t*-ABA was detected in these samples, although some postharvest apple fruits did contain significant amounts of *t*-ABA, as has been reported (3).

In fruit, [^{18}O]ABA was metabolized to [^{18}O]ABA-GE to a much greater extent than it was to [^{18}O]PA, whereas leaves metabolized a larger percentage of ABA to PA than to ABA-GE (Table I). As measured by MS-MS, [^{18}O]ABA-GE (as Me-ABA) did not lose ^{18}O from the carboxyl group during purification or hydrolysis, as evident from the equal ^{18}O enrichment in the side chain of ABA and ABA-GE from the same samples (data not shown). The 4′-keto group of ABA exchanges with water under basic conditions (9), thus [^{18}O]ABA-GE 4′-keto label was lost during hydrolysis and the values of [^{18}O]ABA-GE in Table I are therefore underestimated. In fruits, relatively more [^{18}O]*t*-ABA-GE than [^{18}O]

Table I. *Biosynthesis and Catabolism of ABA in Mutsu Fruit and Leaves under $^{18}O_2$*

Amounts of [^{18}O]ABA and [^{18}O]metabolites synthesized were calculated from the levels measured by GLC-ECD and mutliplied by the percent ^{18}O enrichment as determined by GLC-NCI-SIM of the M^- (Me-ABA, m/z = 280, 282, 284; Me-PA, m/z = 296, 298, 300, 302). No *t*-ABA was detected in these samples.

^{18}O-Labeled Compound	Fruit 48 h $^{18}O_2$	Stressed Leaves 24 h $^{18}O_2$
	ng/g fresh wt/time	
ABA	29.8 ± 6.9[a]	313.0 ± 58.5
PA	0.2 ± 0.1	69.4 ± 14.6
ABA-GE	0.5 ± 0.3	19.8 ± 6.1
t-ABA-GE	3.0 ± 1.3	3.0 ± 0.7

[a] Average of three experiments ± SE.

Table II. *Extent of ABA Functional Group ^{18}O-Labeling in Mutsu Leaf, Immature and Mature Fruit Tissues*

Except for column 3, each class of [^{18}O]ABA molecules is interpreted as having the majority of label in the 1′-hydroxyl group (30).

Tissue/Treatment	Percent of Total [^{18}O]ABA				
	Unlabeled in carboxyl		One ^{18}O atom in carboxyl		
	$(M+2)^-$ 1	$(M+4)^-$ 2	$(M+2)^-$ 3	$(M+4)^-$ 4	$(M+6)^-$ 5
Stressed leaf					
12 h $^{18}O_2$	9.9	Trace	89.4	0.4	0.1
24 h $^{18}O_2$	16.4	Trace	81.4	1.5	0.3
Immature fruit, 48 h $^{18}O_2$					
	42.8	Trace	52.9	0.9	3.3
	30.6	0.1	62.6	2.7	4.0
Mature fruit, 48 h $^{18}O_2$					
5 d postharvest	61.2	0.3	6.8	31.1	0.3
28 d postharvest	64.8	0.6	5.4	29.2	ND[a]
150 d storage[b]	15.1	23.6	17.9	17.8	25.3

[a] Not detected. [b] Stored under hypobaric conditions.

ABA-GE was synthesized; the converse was true for leaves (Table I).

In Table II the various classes of labeled ABA from stressed leaves, immature and mature fruits are expressed as percent of the total [^{18}O]ABA. The class of [^{18}O]ABA containing two ^{18}O atoms in the carboxyl group (30) represented a negligible fraction of total [^{18}O]ABA and is not included in Table II. In all cases examined [^{18}O]ABA not labeled in the carboxyl was completely labeled at the 1′-hydroxyl position. Two aspects of ABA biosynthesis are demonstrated in Table II: the size and turnover of the precursor pool containing oxygen atoms on the ring, and the extent of the proposed carbonyl exchange in an aldehyde which is a precursor to ABA (30). In stressed leaves, the ABA synthesized over 24 h only slightly depleted the precursor pool containing the ring oxygens of ABA (approximately 18% of [^{18}O]ABA contained ^{18}O on the ring after 24 h; see columns 1 + 4 + 5). It can be inferred that there was almost complete exchange of the side chain ^{18}O in a doubly-labeled aldehyde intermediate, because the percent of total [^{18}O]ABA in column 4 is only one-tenth of that in column 1 (Table II). These two classes would be identical at an aldehyde precursor stage before exchange of the side chain carbonyl oxygen with water.

In immature fruit, a larger percentage of ^{18}O-labeled ABA molecules contained ^{18}O atoms on the ring as compared to stressed leaves (approximately 35% compared with < 18% for leaves; combine columns 1, 4, and 5). This suggests that in these fruits the precursor pool containing oxygens on the ring turned over quickly. As in leaves, the proposed exchange of the side chain ^{18}O of an aldehyde intermediate before conversion to ABA was almost complete (compare columns 4 and 1). In mature fruit the majority of labeled ABA molecules contained ^{18}O on the ring. As in the other tissues examined, ^{18}O exchange of an aldehyde precursor was substantial (Table II).

ABA-Aldehyde and ABA-*trans*-Diol in Apple Fruits and Leaves

ABA-aldehyde and ABA-*trans*-diol were present in both fruit and leaf tissues. Figure 2 shows mass spectra of ^{18}O labeled ABA-aldehyde and *t*-ABA-aldehyde isomers separated by GLC. Isomerization, if it occurs *in vivo*, is slow because the two isomers have significantly different ^{18}O enrichment. ABA-aldehyde was synthesized and/or metabolized more quickly than *t*-ABA-aldehyde, as evidenced by the greater ^{18}O enrichment of the *cis* isomer than that of the *trans* isomer (Fig. 2). On the other hand, in three ^{18}O labeling experiments, ABA-*trans*-diol averaged 10% ^{18}O enrichment, while ABA from the same extracts averaged 38% ^{18}O incorporation. Therefore, synthesis and/or turnover of the ABA pool was faster than that of the ABA-*trans*-diol pool in these fruits.

The fragmentation pathways by NCI of ABA-aldehyde and

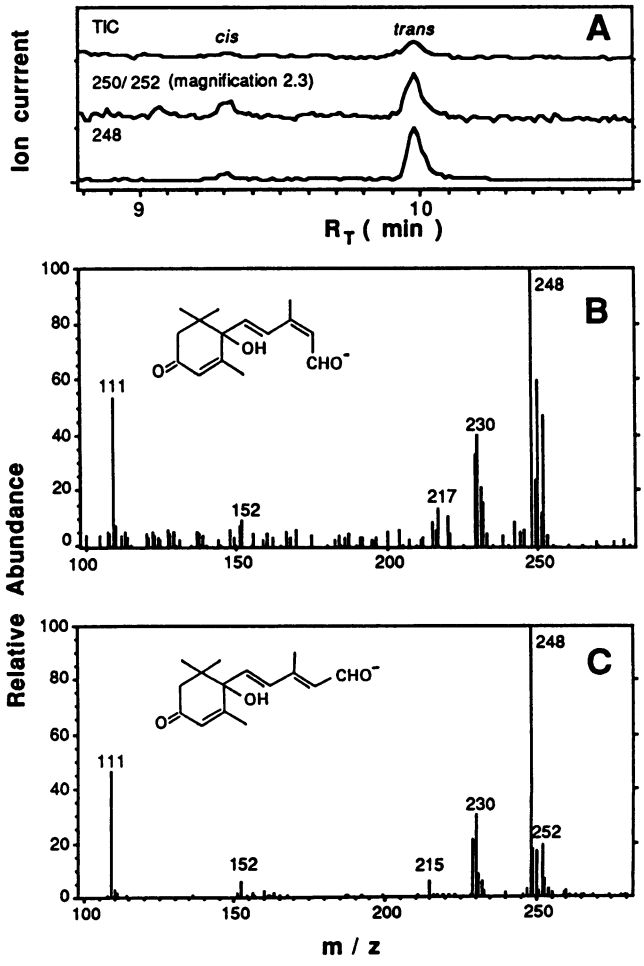

Figure 2. GLC-NCI-MS of apple fruit ABA-aldehyde synthesized under $^{18}O_2$. Granny Smith cortical tissue was incubated for 48 h under $^{18}O_2$. (A) Ion chromatogram with profile of total ion current (TIC), ABA-aldehyde isomer M^-m/z = 248, and ^{18}O-enriched $(M+2)^-$ and $(M+4)^-$, m/z = 250, 252. (B) Mass spectrum of ABA-aldehyde, showing ^{18}O enrichment. R_T = 9 min 18 s. (C) Mass spectrum of *t*-ABA-aldehyde. R_T = 10 min.

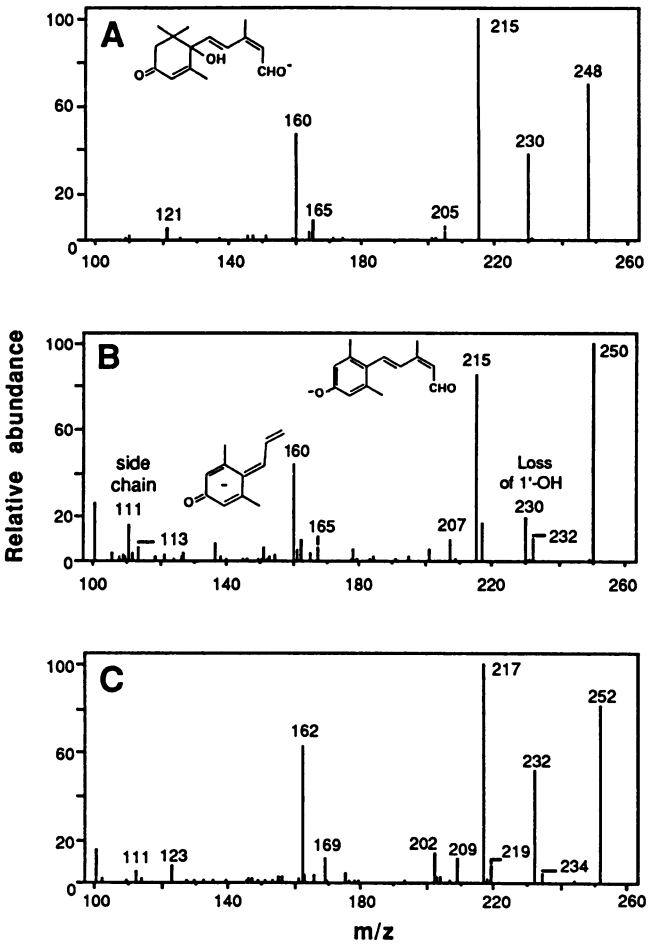

Figure 3. MS-MS of ABA-aldehyde containing zero, one, or two ^{18}O atoms. MS-MS was performed on the sample of Figure 2 to determine the position and extent of ^{18}O incorporation into ABA-aldehyde. ABA-aldehyde and *t*-ABA-aldehyde were not separated by the GLC method employed, so that spectra are of a mixture of ABA-aldehyde isomers. (A) Unlabeled ABA-aldehyde with M^- inset; (B) singly ^{18}O-labeled ABA-aldehydes with fragmentation products inset; (C) doubly ^{18}O-labeled ABA aldehydes.

Me-ABA-*trans*-diol are analogous to those of Me-ABA (19); (C.D. Rock and T.G. Heath, unpublished observations). Figure 3 shows MS-MS spectra obtained from parent M^- of ABA-aldehyde containing zero, one or two ^{18}O atoms. The ion at m/z = 230 corresponds to loss of the 1′-hydroxyl group as water; m/z = 215 has lost the 1′-hydroxyl and a *gem*-methyl group from position C-8′ or C-9′ as methanol. Two other diagnostic ions are m/z = 160, which contains the 4′ keto group, and m/z = 111, which corresponds to the side chain. Measurement of isotope intensities of these ions allows determination of ^{18}O enrichment at each oxygen function of ABA-aldehyde when the parent ions $(M + 2)^-$ (m/z = 250) and $(M + 4)^-$ (m/z = 252) are analyzed by MS-MS.

It is apparent that the side chain carbonyl was only partially ^{18}O-labeled in the $(M + 2)^-$ and $(M + 4)^-$ species (see m/z = 111 and 113; 160 and 162; 215, 217 and 219). The 1′-hydroxyl was predominantly ^{18}O labeled in both the $(M + 2)^-$ and $(M + 4)^-$ species (loss of 20 atomic mass units as $H_2{}^{18}O$; see m/z 230, 232, 234), and the 4′ keto group was partially labeled in the $(M + 2)^-$ and completely labeled in the $(M + 4)^-$ species (see m/z = 162). Thus, the [^{18}O]ABA-aldehyde pool consisted of molecules with ^{18}O at each oxygen function, the majority of the molecules containing ^{18}O in the 1′-hydroxyl group. The ^{18}O incorporation pattern of ABA-aldehyde is correlated with that of [^{18}O]ABA in fruits in which there is lack of label in the side chain and predominant ^{18}O-labeling of the 1′-hydroxyl oxygen (Table II).

In model experiments with synthetic ABA-aldehyde it was established that the carbonyl oxygen of ABA-aldehyde exchanges with H_2O with a half-life of approximately 9 min (± 2 SE, $n = 9$), but does not exchange ^{18}O carbonyl label when dissolved in ethyl acetate (data not shown). Rapid workup and phase partitioning of aqueous extracts from ^{18}O-labeled tissue may have allowed retention of some label in the carbonyl oxygen of ABA-aldehyde from ^{18}O-labeled samples (Fig. 3, Table III).

In Table III the percent ^{18}O-enrichment in the side chain is compared between ABA-aldehyde, ABA, and ABA-*trans*-diol extracted from the same sample and analyzed by MS-MS. The law of mass action supports a precursor role for species which have a higher specific activity of ^{18}O label than the product, assuming biosynthetic precursor pools are homogeneous and the label does not exchange with the medium. The second assumption is true for the carboxyl and 1′-hydroxyl groups of ABA (6), but not for the carbonyl of ABA-aldehyde, which exchanges oxygen with water (see above). The 4′-keto group of ABA can slowly exchange with water with a half-life of days (6). ABA-*trans*-diol can slowly exchange the 1′-hydroxyl with water, but not the 4′-hydroxyl (27). Because each compound can exchange some oxygen function with water, the ^{18}O labeled $(M + 4)^-$ pools are converted to the $(M + 2)^-$ pools for each compound. Thus, the weighted average of side chain enrichment (factoring in the relative abundance of each M^-) is presented in Table III. Taking into account the loss of

Table III. *^{18}O Incorporation in the Side Chain of ABA-Aldehyde, ABA-trans-Diol and ABA Extracted from the Same Fruit Sample after 48 h under $^{18}O_2$*

Percent side chain enrichment was calculated from intensities of daughter ions measured by MS-MS and GLC-NCI-SIM of ^{18}O-enriched M^- (Me-ABA m/z = 280, 282, 284; Me-ABA-*trans*-diol m/z = 282, 284; ABA-aldehyde m/z = 250, 252). ABA-aldehyde was measured as a mixture of *cis*- and *trans*-isomers. Experiments 1 to 4 were performed with post-harvest Granny Smith cortex tissue, experiment 5 with Mutsu cortex from fruits stored under hypobaric conditions.

Experiment	Percent of ^{18}O-Labeled Molecules Containing ^{18}O in the Side Chain		
	ABA-aldehydes	ABA	ABA-*trans*-diol
1	18.2	10.6	6.1
2	13.6	16.0	4.1
3	10.5	71.8	5.5
4	NA[a]	42.0	25.5
5	NA	59.4	35.2

[a] Not analyzed.

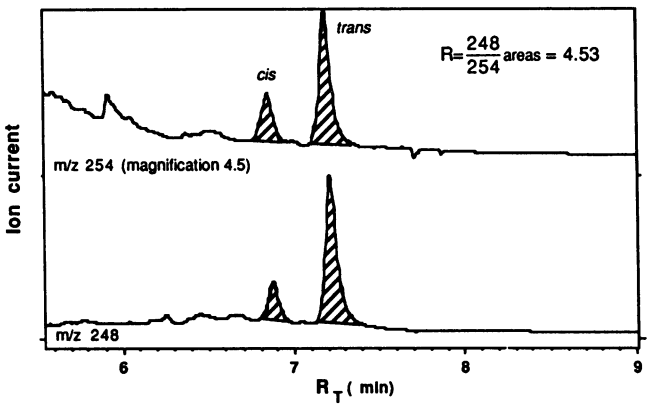

Figure 4. GLC-NCI-SIM chromatogram of ABA-aldehyde from Mutsu fruit with [$^2H_6$]ABA-aldehyde internal standard. The sum of the ABA-aldehyde plus *t*-ABA-aldehyde peak areas gave a ratio of unlabeled to [$^2H_6$]ABA-aldehyde, from which the amount of unknown endogenous ABA-aldehyde was calculated.

^{18}O label from the ABA-aldehyde side chain carbonyl due to exchange with the medium, a precursor role of ABA-aldehyde for ABA can be inferred. In one experiment the side chain label of ABA-aldehyde was actually higher than that of ABA. In all cases the side chain specific activity of Me-ABA (percent ^{18}O in side chain of total ^{18}O) was greater than that of Me-ABA-*trans*-diol. Thus, these data suggest that ABA is a precursor to ABA-*trans*-diol.

Quantification of ABA-Aldehyde and ABA-*trans*-Diol

The method of isotope dilution of deuterated internal standards (17) was used to quantify ABA-aldehyde and ABA-*trans*-diol. Retention and stability of deuterium label during extraction and purification procedures were confirmed by dissolving deuterium-labeled compounds in 0.2 M phosphate buffers, ranging from pH 3.5 to 10, for 6 d at room temperature, followed by partitioning into ethyl acetate and analysis by GLC-MS. There was less than 1% exchange of deuterium for both standards over the range of pHs tested (data not shown). Thus, the internal standards could be used for quantification, provided the standards were added at concentrations less than five times the endogenous sample concentrations to minimize contamination of the nominal mass peak by unlabeled internal standard (see "Materials and Methods").

Figure 4 shows a GLC-NCI-SIM chromatogram for quantification of ABA-aldehyde. The deuterated material eluted from the GLC column about 2 s earlier than the unlabeled compound. The ratio of ABA-aldehyde to *t*-ABA-aldehyde as measured by NCI-SIM was essentially constant, regardless of the actual quantities of isomers present in a stock solution. This suggested that the two isomers were not equally detected by this method. Consequently, both isomers were then analyzed by various GLC detection methods. In Table IV the phenomenon of 'differential ionization' of ABA-aldehyde isomers is illustrated. FID generates a signal based on the mass and organic composition of the compound being measured and is unbiased in the response toward different isomers of similar or identical compounds. Positive ion detection methods (PCI and EI) generally reflected the abundance of ABA-aldehyde versus *t*-ABA-aldehyde isomers, but were relatively less sensitive to ABA-aldehyde than FID. NCI and ECD consistently gave ABA-aldehyde to *t*-ABA-aldehyde isomer ratios which were less than unity, indicating that the two isomers were differentially ionized. The degree of ABA-aldehyde ionization was affected by the pressure of reagent gas (Table IV). The mechanism of this differential ionization is unknown. Thermal isomerization of ABA-aldehyde in the injection port of the gas chromatograph was ruled out as a possible cause of observed isomer ratios (see Fig. 3). Xanthoxin and *t*-xanthoxin ratios were relatively constant regardless of the detection method employed (Table IV), even though the chemical structure is quite similar to that of ABA-aldehyde. NCI was the only mass spectroscopy method tested which was sensitive enough to measure the small amounts of ABA-aldehyde present in plants. It was apparent that ABA-aldehyde isomers could not be quantified by NCI-SIM using a deuterated internal standard because the *cis* isomer was refractory to ionization. The relative amount of *cis* isomer was reflected in the NCI-MS signal at high reagent gas pressure (Table IV). Because the ratio of *cis*- to *trans*-ABA-aldehyde isomers in the deuterated internal standard was known, and the endogenous isomer ratio was similar (Fig. 4), the sum of the two isomer concentrations was used as a measure of total ABA-aldehydes.

In Table V the levels of ABA, ABA-*trans*-diol and ABA-aldehyde plus *t*-ABA-aldehyde in leaves and apple fruit tissue are presented. There was very little ABA-*trans*-diol in either leaves or fruit, and no ABA-alcohol was detected. ABA-aldehyde levels were low in all tissues examined. When ABA-aldehyde concentrations are presented as percent of ABA levels, there is a trend toward relatively higher ABA-aldehyde levels from leaves to mature fruits (Table V).

Feeding Studies with Deuterated Substrates

Table VI summarizes feeding experiments addressing the biosynthetic relationship of putative ABA precursors. [$^2H_6$]ABA-aldehyde and and [$^2H_6$]*t*-ABA-aldehyde were converted to [$^2H_6$]ABA and [$^2H_6$]*t*-ABA, which were further converted

Table IV. *Comparison of cis- and trans-ABA-Aldehyde and -Xanthoxin Isomer Ratios by Various GLC Detection Methods*

An aliquot of a stock solution was chromatographed by GLC using a DB-1 capillary column and the isomers quantified by peak areas of the detector responses. For mass spectrometric detection methods, the total ion current was integrated.

Sample	Ratio of *cis* to *trans* Isomer Areas					
	FID	PCI	EI	NCI_{LOW}[a]	NCI_{HIGH}[a]	ECD
ABA-aldehyde	55.4	10.9	2.3	0.5	0.9	1.1
cis- and *trans*-ABA-aldehydes	0.6	0.2	0.2	0.2	0.3	0.2
[$^2H_6$]ABA-aldehydes	5.1	1.1	1.0	0.2	0.4	0.8
cis- and *trans*-xanthoxins	0.3	0.3	0.4	0.3	0.3	0.4

[a] Methane chemical ionization gas pressure was 6.7×10^{-4} and 2.0×10^{-3} Pa for "low" and "high" measurements, respectively.

Table V. *Quantification of ABA, ABA-trans-Diol and cis- plus trans-ABA-Aldehydes in Mutsu Fruit and Leaves*

ABA was quantified by GC-ECD using [^{3}H]ABA as an internal standard. ABA-aldehydes and ABA-*trans*-diol were quantified by isotope dilution using ^{2}H-labeled synthetic standards and measurement by GLC-NCI-SIM of the M^- as shown in Figure 4.

Tissue	Sample			$\frac{\text{ABA-Aldehydes}}{\text{ABA}} \times 100$
	ABA	ABA-*trans*-diol	ABA-aldehydes (*cis* + *trans*)	
	ng/g fr wt			%
Unstressed leaf	362.80[a]	0.02	1.02	0.3
Immature fruit[a]	19.85	NA[b]	0.44	2.2
Mature fruit[c]	5.12	0.01	0.68	13.3

[a] Average of two experiments. [b] Not analyzed. [c] Average of four experiments.

to [$^2H_6$]ABA-GE and [$^2H_6$]*t*-ABA-GE. There was no evidence for isomerization of ABA to *t*-ABA (Table VI, [$^2H_7$]ABA-*trans*-diol feed), or ABA-GE to *t*-ABA-GE ([$^2H_6$]ABA feed) during the incubation. These data can be interpreted as showing a direct conversion of ABA-aldehyde to ABA to ABA-GE, and of *t*-ABA-aldehyde to *t*-ABA to *t*-ABA-GE. The rate of metabolism of *t*-ABA to *t*-ABA-GE appears to be greater than that of ABA to ABA-GE, as indicated by the lower levels of *t*-ABA relative to ABA and higher levels of *t*-ABA-GE than of ABA-GE. A higher rate of conjugation for *t*-ABA than for ABA has been reported for other plants (16). The (−) enantiomer of ABA is conjugated readily (16); thus, a significant proportion of the [^{2}H]ABA-GE product would be (−)-ABA-GE, if (−)-ABA-aldehyde was converted to (−)-ABA. The conclusions reached for conversion of [$^2H_6$]ABA-aldehyde to ABA and ABA-GE isomers also hold for the [$^2H_6$]ABA-alcohol feeding experiment. Assuming the applied compounds entered the cell to equal extents and were not converted to products other than listed in Table VI, it can be concluded that the rate of metabolism of [$^2H_6$]ABA-alcohol was slower than that of [$^2H_6$]ABA-aldehyde.

Conversion of [$^2H_7$]ABA-*trans*-diol to ABA took place; however, this oxidation occurred nonenzymatically as evidenced by the presence of [$^2H_6$]ABA in the autoclaved control feed (see also ref. 27). [$^2H_6$]ABA was enzymatically reduced to [$^2H_6$]ABA-*trans*-diol (Table VI). The extent of this conversion was dependent on the concentration of ABA. When [$^2H_6$]ABA was fed at a concentration approximately 400-fold higher than the endogenous ABA level, the [$^2H_6$]ABA-*trans*-diol produced was about 50 times the endogenous ABA-*trans*-diol content; quantifications of ABA-*trans*-diol also support a concentration dependence on ABA (Table V).

Table VI. *Metabolism of Deuterated Compounds Fed to Mutsu Fruit Tissue*

Plugs of cortex tissue (1.4 cm diameter) were vacuum-infiltrated with 2 mL of a 10 μM solution of substrate (except [$^2H_7$]ABA-*trans*-diol, 2.0 μM). The substrates [$^2H_6$]ABA-aldehyde and [$^2H_6$]ABA-alcohol contained a significant amount of the respective *trans* isomer. The control tissue was autoclaved before addition of substrate for the 48 h incubation period.

Substrate	Product				
	[^{2}H]ABA	[^{2}H]*t*-ABA	[^{2}H]ABA-*trans*-diol	[^{2}H]ABA-GE	[^{2}H]*t*-ABA-GE
			ng/g fresh wt/time		
[$^2H_6$]ABA-aldehyde					
24 h	1.6	0.2		ND	2.6
48 h	1.4	1.1		1.6	8.0
Control	ND[a]	ND		ND	ND
[$^2H_6$]ABA-alcohol					
24 h	0.2	ND		ND	0.3
48 h	0.8	ND		ND	3.4
Control	ND	ND		ND	ND
[$^2H_7$]ABA-*trans*-diol					
24 h	7.1	ND		0.2	0.1
48 h	5.3	ND		3.2	0.1
Control	12.5	ND		ND	ND
[$^2H_6$]ABA					
24 h			0.4	2.0	ND
48 h			0.6	17.3	ND
Control			ND	ND	ND

[a] Not detected.

DISCUSSION

ABA-Aldehyde as a Precursor to, and ABA-*trans*-Diol as a Catabolite of ABA

Evidence is presented that ABA-aldehyde is the immediate precursor to ABA, and that ABA-*trans*-diol is a catabolite of ABA in apple fruits and leaves, and possibly in all plants. These conclusions are based on the following evidence. (a) Assuming the labeled and unlabeled metabolite pools were in equilibrium, there was greater flux through the ABA-aldehyde pool than the *t*-ABA-aldehyde pool (Fig. 2). These data are consistent with an enzymatic specificity toward the *cis* isomer of ABA, the biologically active isomer in plants (28). There was also greater flux through the ABA *versus* ABA-*trans*-diol pools (data not shown), which supports ABA as a precursor to ABA-*trans*-diol. (b) Precursor-product relationships were established by measurement of ^{18}O specific activity of metabolites extracted from ^{18}O-labeled tissues (Table III), and by feeding studies using deuterated substrates (Table VI). (c) There were low endogenous levels of ABA-aldehyde and ABA-*trans*-diol (Table V) and a concentration dependence of ABA-*trans*-diol on ABA.

ABA-aldehyde has been postulated as a precursor to ABA, because the ABA-deficient *flacca* and *sitiens* mutants of tomato are unable to convert xanthoxin or ABA-aldehyde to ABA *in vivo* (21, 25) or *in vitro* (23). Taylor *et al.* (15, 25) showed that these mutants reduce ABA-aldehyde to *t*-ABA-alcohol, which accumulates to high levels. [$^2H_6$]ABA-alcohol is converted to ABA in apple fruits, but at lower rates than [$^2H_6$]ABA-aldehyde (Table VI).

ABA Biosynthesis in Apple Fruits and Leaves

The qualitative and quantitative data obtained by MS-MS of metabolites from ^{18}O-labeled tissues provide a means to analyze the ABA biosynthetic pathway, especially rates of turnover of precursor pools. Two conclusions can be drawn from Table II regarding the precursor(s) of ABA. (a) Based on ABA biosynthetic capacity of the tissues (Table I), and the turnover rate of the pools as judged by ^{18}O incorporation on the ring of ABA (Table II), the precursor pool containing ring oxygens is large in leaves and much smaller in fruits. (b) In apple, and perhaps in all plants, a significant amount of exchange occurs between the medium and the carbonyl side chain oxygen of an aldehyde precursor to ABA. This carbonyl exchange would give rise to unlabeled ABA synthesized under $^{18}O_2$ in tissues which have a large precursor pool. ABA labeled exclusively in the ring oxygens is observed only in tissues (like apple fruit) which have a small, rapidly depleted violaxanthin precursor pool. This tissue type synthesizes ABA labeled in the ring oxygen functions, but without label in the carboxyl group. The exchange can be at the ABA-aldehyde level (Fig. 3), but could also occur in an aldehyde precursor prior to ABA-aldehyde, such as xanthoxin. Parry *et al.* (21) observed a low amount of ^{18}O incorporation from $^{18}O_2$ into xanthoxin in tomato leaves and suggested that lack of steady state ^{18}O enrichment might be due to carbonyl exchange.

ABA biosynthesis and catabolism in climacteric fruits is under developmental control, in contrast to leaves where turgor pressure is a regulatory signal for ABA metabolism (29). The regulation of ABA biosynthesis and catabolism is different in leaves and fruits; hydroxylation of ABA to PA is a minor pathway in fruits (Table I), but the major catabolic pathway in leaves (Table I) (29). Fruits synthesize relatively more of the *trans* than the *cis* isomer of ABA-GE; in contrast, leaves synthesize more ABA-GE than *t*-ABA-GE (Table I). There is no evidence to support enzymatic isomerization of ABA to *t*-ABA, or of ABA-GE to *t*-ABA-GE (Table VI) (16). We hypothesize that ABA and *t*-ABA biosynthesis and metabolism proceed in parallel from xanthophylls to xanthoxin isomers, through ABA-aldehyde isomers, to the corresponding isomers of ABA and ABA-GE. Both *cis*- and *trans*-xanthoxin isomers are present in plants, and *t*-xanthoxin is converted to *t*-ABA (16, 21, 22). Sindhu and Walton (23) showed that bean leaf extracts convert ABA-aldehyde and *t*-ABA-aldehyde predominantly to ABA and *t*-ABA, respectively. If the levels of ABA-aldehyde plus *t*-ABA-aldehyde are similar in leaves and fruits, but ABA levels are much lower in fruits (Table V), then the latter should contain more *t*-ABA-aldehyde than leaves. The relatively high *t*-ABA-GE levels in fruits are evidence in support of this hypothesis. The large amounts of *t*-ABA found in apple fruits (3) may not have been due to isomerization as proposed, but by a loss of ABA-conjugating activity in these apples. A precise measurement of ABA-aldehyde and *t*-ABA-aldehyde levels would provide further insight into synthesis of ABA and *t*-ABA in plants.

ACKNOWLEDGMENTS

We thank T.G. Heath and Dr. D.A. Gage for assistance with mass spectrometry, Dr. D.R. Dilley and Dr. F.G. Dennis Jr. for providing plant material, and Dr. M. Soukup, Hoffmann-LaRoche, Inc. for providing synthetic ABA-alcohol and ABA-aldehyde.

LITERATURE CITED

1. **Adams DO, Yang SF** (1979) Ethylene biosynthesis: identification of 1-aminocyclopropane-1-carboxylic acid as an intermediate in the conversion of methionine to ethylene. Proc Natl Acad Sci USA **76**: 170–174
2. **Adato I, Gazit S, Blumenfeld A** (1976) Relationship between changes in abscisic acid and ethylene production during ripening of avocado fruits. Aust J Plant Physiol **3**: 555–558
3. **Bangerth F** (1982) Changes in the ratio of *cis-trans* to *trans-trans* abscisic acid during ripening of apple fruits. Planta **155**: 199–203
4. **Boyer GL, Zeevaart JAD** (1982) Isolation and quantitation of β-D-glucopyranosyl abscisate from leaves of *Xanthium* and spinach. Plant Physiol **70**: 227–231
5. **Cornish K, Zeevaart JAD** (1984) Abscisic acid metabolism in relation to water stress and leaf age in *Xanthium strumarium*. Plant Physiol **76**: 1029–1035
6. **Creelman RA, Gage DA, Stults JT, Zeevaart JAD** (1987) Abscisic acid biosynthesis in leaves and roots of *Xanthium strumarium*. Plant Physiol **85**: 726–732
7. **Creelman RA, Zeevaart JAD** (1984) Incorporation of oxygen into abscisic acid and phaseic acid from molecular oxygen. Plant Physiol **75**: 166–169
8. **Gamble PE, Mullet JE** (1986) Inhibition of carotenoid accumulation and abscisic acid biosynthesis in fluridone-treated dark-grown barley. Eur J Biochem **160**: 117–121
9. **Gray RT, Mallaby R, Ryback G, Williams VP** (1974) Mass spectra of methyl abscisate and isotopically labeled analogs. J Chem Soc Perkins Trans 2: 919–924

10. **Gritter RJ, Wallace TJ** (1959) The manganese dioxide oxidation of allylic alcohols. J Org Chem **24**: 1051–1056
11. **Hirai N, Okamoto M, Koshimizu K** (1986) The 1′,4′-*trans*-diol of abscisic acid, a possible precursor of abscisic acid in *Botrytis cinerea*. Phytochemistry **25**: 1865–1868
12. **Kende H, Hanson AD** (1975) Relationship between ethylene evolution and senescence in morning-glory flower tissue. Plant Physiol **57**: 523–527
13. **Li Y, Walton DC** (1987) Xanthophylls and abscisic acid biosynthesis in water-stressed bean leaves. Plant Physiol **85**: 910–915
14. **Li Y, Walton DC** (1990) Violaxanthin is an ABA precursor in water-stressed dark-grown bean leaves. Plant Physiol **92**: 551–559
15. **Linforth RST, Bowman WR, Griffin DA, Marples BA, Taylor IB** (1987) 2-*trans*-ABA-alcohol accumulation in the wilty tomato mutants *flacca* and *sitiens*. Plant Cell Environ **10**: 599–606
16. **Milborrow BV** (1983) Pathways to and from abscisic acid. *In* FT Addicott, ed, Abscisic Acid. Praeger, New York, pp 79–111
17. **Neill SJ, Horgan R** (1987) Abscisic acid and related compounds. *In* L Rivier, A Crozier, eds, Principles and Practice of Plant Hormone Analysis, Vol 1. Academic, London, pp 111–167
18. **Neill SJ, Horgan R, Parry AD** (1986) The carotenoid and abscisic acid content of viviparous kernels and seedlings of *Zea mays* L. Planta **169**: 87–96
19. **Netting AG, Milborrow BV, Vaughan GT, Lidgard RO** (1988) The fragmentation of methyl abscisate and its 2*E* isomer in methane positive and negative chemical ionization mass spectrometry. Biomed Environ Mass Spectrom **15**: 375–389
20. **Okamoto M, Hirai N, Koshimizu K** (1987) Occurrence and metabolism of 1′,4′-*trans*-diol of abscisic acid. Phytochemistry **26**: 1269–1271
21. **Parry AD, Neill SJ, Horgan R** (1988) Xanthoxin levels and metabolism in the wild-type and wilty mutants of tomato. Planta **173**: 397–404
22. **Sindhu RK, Walton DC** (1987) Conversion of xanthoxin to abscisic acid by cell-free preparations from bean leaves. Plant Physiol **85**: 916–921
23. **Sindhu RK, Walton DC** (1988) Xanthoxin metabolism in cell-free preparations from wild type and wilty mutants of tomato. Plant Physiol **88**: 178–182
24. **Taylor HF, Burden RS** (1972) Xanthoxin, a recently discovered plant growth inhibitor. Proc R Soc Lond Ser B **180**: 317–346
25. **Taylor IB, Linforth RST, Al-Naieb RJ, Bowman WR, Marples BA** (1988) The wilty mutants *flacca* and *sitiens* are impaired in the oxidation of ABA-aldehyde to ABA. Plant Cell Environ **11**: 739–745
26. **Vaughan GT, Milborrow BV** (1987) The occurrence and metabolism of the 1′,4′-diols of abscisic acid. Aust J Plant Physiol **14**: 593–604
27. **Vaughan GT, Milborrow BV** (1988) The stability of the 1′,4′-diols of abscisic acid. Phytochemistry **27**: 339–343
28. **Walton DC** (1983) Structure-activity relationships of abscisic acid analogs and metabolites. *In* FT Addicott, ed, Abscisic Acid. Praeger, New York, pp 113–146
29. **Zeevaart JAD, Creelman RA** (1988) Metabolism and physiology of abscisic acid. Annu Rev Plant Physiol Plant Mol Biol **39**: 439–473
30. **Zeevaart JAD, Heath TG, Gage DA** (1989) Evidence for a universal pathway of abscisic acid biosynthesis in higher plants from ^{18}O incorporation patterns. Plant Physiol **91**: 1594–1601